Author Manuscript

Author Manuscript

Author Manuscript

Author Manuscript

HHS Public Access

Author manuscript

Nat Med. Author manuscript; available in PMC 2009 December 01.

Published in final edited form as:

Nat Med. 2009 June ; 15(6): 682–689. doi:10.1038/nm.1954.

Inhibition of Osteoblast Functions by IKK/NF-κB in Osteoporosis

Jia Chang[1], **Zhuo Wang**[2], **Eric Tang**[1], **Zhipeng Fan**[1], **Laurie McCauley**[3,4], **Renny Franceschi**[3], **Kunliang Guan**[5], **Paul H. Krebsbach**[2], and **Cun-Yu Wang**[1,*]

[1]Lab of Molecular Signaling, Division of Oral Biology and Medicine, School of Dentistry and Jonsson Comprehensive Cancer Center, UCLA, Los Angeles, CA 90095, USA

[2]Department of Biologic and Materials Sciences, The University of Michigan, Ann Arbor, MI 48109

[3]Department of Periodontics and Oral Medicine, School of Dentistry, The University of Michigan, Ann Arbor, MI 48109

[4]Department of Pathology, School of Medicine, The University of Michigan, Ann Arbor, MI 48109

[5]Department of Pharmacology and Comprehensive Cancer Center, UCSD, San Diego, CA 92093

Abstract

An imbalance in bone formation relative to bone resorption results in the net bone loss in osteoporosis and inflammatory bone diseases. While it is well known how bone resorption is stimulated, the molecular mechanisms that mediate impaired bone formation are poorly understood. Here we show that the time- and stage-specific inhibition of endogenous IκB kinase (IKK)/nuclear factor-kappa B (NF-κB) NF-κB in differentiated osteoblasts significantly increases trabecular bone mass and bone mineral density without affecting osteoclast activities in young mice. Moreover, the inhibition of IKK/NF-κB in differentiated osteoblasts maintains bone formation, thereby preventing osteoporotic bone loss induced by ovariectomy (OVX) in adult mice. The inhibition of IKK/NF-κB enhances the expression of Fra-1, an essential factor for bone matrix formation *in vitro* and *in vivo*. Taken together, our results suggest that targeting IKK/NF-κB may help to promote bone formation in the treatment of osteoporosis and other bone diseases.

Postnatal skeletal growth and bone remodeling are highly coordinated processes that are primarily mediated by bone-forming osteoblasts and bone-resorbing osteoclasts1-3. To maintain normal bone homeostasis, bone resorption is delicately balanced with bone extracellular matrix deposition or bone formation, ensuring that new bone is generated

Users may view, print, copy, and download text and data-mine the content in such documents, for the purposes of academic research, subject always to the full Conditions of use:http://www.nature.com/authors/editorial_policies/license.html#terms

*To whom correspondence should be addressed, Dr. Cun-Yu Wang, Laboratory of Molecular Signaling, UCLA, 10833 Le Conte Ave., Los Angeles, CA 90095, Phone: 310-825-4415, Fax: 310-794-7109, Email: cwang@dentistry.ucla.edu.

AUTHOR CONTRIBUTIONS

J.C. performed the majority of the experiments, analyzed data and prepared figures. Z.W. performed μCT and analyzed data. E.T. performed cDNA subcloning. Z.F. performed cDNA subcloning. L.M. helped experiment designs and the preparation of manuscript. R.F. provided reagents and helped the preparation of manuscript. K.G. provided reagents and helped the preparation of manuscript. P.H.K. helped with μCT and the preparation of manuscript.

COMPETING INTERESTS STATEMENT

The authors declare that they have no competing financial interests.

Author Manuscript Author Manuscript Author Manuscript Author Manuscript

where old bone is removed1,4-6. Sex steroid deficiency following menopause is a frequent cause of osteoporosis that is characterized by trabecular bone loss and increased risk of fracture. Osteoporosis is the most common metabolic bone disease and a leading cause of morbidity and mortality in our aging population. It is commonly believed that bone formation is significantly impaired in osteoporosis which is partially responsible for a net bone loss7-11. Also, bone formation is substantially compromised in inflammatory bone diseases such as arthritis and periodontitis8. Thus, understanding how the function of differentiated or mature osteoblasts is regulated in postnatal life is important for developing novel and improved strategies for treating osteoporosis and inflammatory bone diseases.

The transcription factor nuclear factor kappa B (NF-κB) plays a critical role in inflammation and immune responses12-16. Growing evidence suggests that NF-κB signaling may be associated with metabolic diseases such as cachexia and diabetes17-19. The inhibition of IKKβ by specific peptides suppressed inflammatory bone loss by inhibiting osteoclast formation in an arthritis model, suggesting that NF-κB is an important target for the treatment of inflammatory bone diseases18. However, although the actions of NF-κB on osteoclastogenesis are well-understood19, little is currently known about possible actions of NF-κB on osteoblast activity and bone formation, especially at the stage of postnatal skeletal growth and bone remodeling. In this study, we found that NF-κB activation in differentiated osteoblasts has an anti-anabolic effect on bone formation. We uncovered that NF-κB is a critical factor responsible for impaired bone formation in osteoporosis. The specific inhibition of NF-κB in differentiated osteoblasts significantly prevented bone loss in ovariectomized (OVXed) mice by maintaining bone formation.

RESULTS

Inhibition of NF-κB in mature osteoblasts promotes postnatal bone formation *in vivo*

Our initial study was to investigate whether NF-κB also regulates osteoblast differentiation of mesenchymal cells since NF-κB was found to play an essential role in osteoclastogenesis19. Using two different NF-κB inhibitors, the dominant negative mutant of IKK-γ (IKK-DN or IKKγC417R) and super-repressor of IκBα (SR-IκBα)20-24, we found that the inhibition of NF-κB enhanced osteoblastic differentiation of mesenchymal C2C12 cells in vitro (Supplementary Fig. S1). Skeletal growth and bone remodeling are dynamic processes in postnatal life1,2,25. While significant progress has been made in understanding the molecular control of osteoblast differentiation during embryonic development, how the function of mature osteoblasts in postnatal life is regulated is not well studied. Due to cell heterogeneity, it is very difficult to distinguish whether NF-κB affects osteoblast differentiation or function in vitro. Since gene ablation of major IKK/NF-κB components in mice results in an embryonic lethality, it is impossible to use these mice to examine the role of NF-κB in bone formation in various bone disease models. Based on our results from mesenchymal cells, we took advantage of the osteoblast-specific bone gamma-carboxyglutamate protein 2 (*Bglap2*) promoter which has been shown to be specifically activated in mature or differentiated osteoblasts and to be inactive in osteoblast progenitors26-28. Our strategy was to use the *Bglap2* promoter to drive IKK-DN in mature osteoblasts so that we could address whether NF-κB regulates mature osteoblast function

Author Manuscript Author Manuscript Author Manuscript Author Manuscript

without affecting osteoblast differentiation. We generated an IKK-DN construct under the control of the *Bglap2* promoter. As expected, this construct was active in ROS17/2.8 osteoblast-like osteosarcoma cells, but was inactive in 293T cells. As a positive control, CMV-driving IKK-DN was expressed in 293T cells (Fig. 1a). Subsequently, we utilized this construct to generate *Bglap2*-IKK-DN transgenic mice. Southern blot analysis revealed six founders expressing the transgene (Fig. 1b). One of the founders which expressed multiple copies of IKK-DN (Fig. 1b, lane 3) died shortly after birth. We maintained and utilized two different transgenic mouse lines (TG1 and TG2) for further experiments. We detected IKK-DN proteins in transgenic mice in bone extracts, but not in other tissues including brain, liver, and muscle (Fig. 1c). Moreover, we isolated calvarial cells from two transgenic mouse lines. While IKK-DN could not be detected in freshly isolated calvarial cells, IKK-DN was induced in cells from *Bglap2*-IKK-DN mice after 2 weeks, but not in cells from wild type littermates (WT; Fig. 1d). Not surprisingly, as shown in Fig. 1e, the *Bglap2*-IKK-DN mouse had a phenotypically normal skeleton at birth. Histological sections also confirmed that both *Bglap2*-IKK-DN mice and WT mice had normal bone structures (data not shown).

To examine whether the inhibition of NF-κB affected postnatal bone formation, we followed mouse skeletal growth of two transgenic founder lines by microradiography and μCT. X-ray showed that the size of *Bglap2*-IKK-DN mice has not significantly different from that of wild type mice (data not shown). However, μCT analysis of the secondary spongiosa of distal femur metaphyses revealed that the bone mineral density (BMD) in the trabecular bone of *Bglap2*-IKK-DN mice was significantly increased compared with control mice at the age of 2 and 4 weeks, but not 2 and 6 months (Fig. 2a and b). Similarly, bone volumes (BV/TV) were also increased in *Bglap2*-IKK-DN mice compared with control mice at the age of 2 and 4 weeks, but not 2 and 6 months (Fig. 2a and b). However, there was no significant difference in cortical bone volume between the two groups (data not shown). Histological analysis of femurs and von Kossa staining of tibiae confirmed that the trabecular bone areas were significantly increased in 2-week-old *Bglap2*-IKK-DN mice compared with WT mice (Fig. 2c and d), suggesting that the inhibition of NF-κB enhances osteoblast function. The number of osteoblasts was similar in both *Bglap2*-IKK-DN mice and control mice, indicating that the inhibition of NF-κB in mature osteoblasts does not affect osteoblast differentiation (Fig. 2e). To further confirm that increased BMD was due to enhanced osteoblast function, we performed dynamic histomorphometric analysis over a 7-day period using calcein labeling, a well-known marker of bone formation. The bone formation rate in 2-week-old *Bglap2*-IKK-DN mice (477 ± 89 $\mu m^3/\mu m^2$/year) was a 1.6-fold increase than that in control WT mice (299 ± 59 $\mu m^3/\mu m^2$/year) (Fig. 2f). Real-time RT-PCR revealed that the levels of bone matrix genes including *Col1α1*, *Col1α2*, *Ocn*, and *Ibsp* were increased in bone extracts of 2- or 4-week-old *Bglap2*-IKK-DN mice (Fig. 2g). To examine whether the inhibition of NF-κB in differentiated osteoblasts affected osteoclast indirectly, we performed tartrate-resistant acid phosphatase (TRAP) assay. The number of osteoclasts was similar in both *Bglap2*-IKK-DN mice and WT mice (Fig. 2h). The level of serum TRAP5b, a sensitive marker of bone resorption and osteoclast function8,11, was similar in both mice (Fig. 2i), suggesting that the inhibition of NF-κB in mature osteoblasts does not affect osteoclast activation and bone resorption. Additionally, we also used the 2.3-kilobase *Col1α1* promoter to drive IKK-DN expression in early differentiated osteoblasts in

Author Manuscript Author Manuscript Author Manuscript Author Manuscript

mice (*Col1α1*-IKK-DN mice). Like *Bglap2*-IKK-DN mice, BMD and trabecular bone formation in young mice were also significantly enhanced as determined by μCT and histological analysis (Supplementary Fig. S2). Taken together, these results suggest that the inhibition of NF-κB in differentiated osteoblasts promotes bone formation in young mice.

IKK/NF-κB inhibition increases bone formation in a cell-autonomous manner

To specifically determine if the inhibition of NF-κB enhanced bone-forming activity of osteoblasts by a cell-autonomous effect, we isolated primary calvarial cells from both *Bglap2*-IKK-DN mice and WT mice. TNF induced similar kinetics of IκBα phosphorylation and degradation in newly-isolated calvarial cells from *Bglap2*-IKK-DN and WT mice (Fig. 3a). To determine whether IKK-DN blocked NF-κB in differentiated osteoblasts, we grow cells in differentiation-inducing medium for 10 days and then treated with TNF. Western blot confirmed that the expression of IKK-DN was induced in differentiated osteoblasts (Fig. 3b). While TNF induced phosphorylation and degradation of IκBα in WT cells, these events were significantly inhibited in differentiated *Bglap2*-IKK-DN cells (Fig. 3b). Additionally, the phosphorylation of p65 at Ser536, a well-known site of IKKβ action21 was also significantly inhibited (Fig. 3b). Electrophoretic mobility shift assay (EMSA) and Western blot analysis also confirmed that the induction of IKK-DN inhibited the nuclear translocation of the NF-κB induced by TNF in *Bglap2*-IKK-DN cells (Fig. 3c,d). The super-shift assay demonstrated that NF-κB-binding activities in differentiated osteoblasts mainly consisted of p65 and p50 (Fig. 3d). Moreover, we found that osteoblast differentiation induced NF-κB binding activity in both *Bglap2*-IKK-DN cells and WT cells to a similar degree at the early time points. However, NF-κB binding activity were suppressed in *Bglap2*-IKK-DN cells 2 weeks after the induction of differentiation, validating that IKK-DN inhibited NF-κB in differentiated osteoblasts (Fig. 3e). NF-κB binding activity in differentiated osteoblasts did not contain c-Rel and RelB (Supplementary Fig. S3). Upon induction of differentiation, bone matrix mineralization was more dramatically enhanced in *Bglap2*-IKK-DN cells compared to that in WT cells (Fig. 3f). Consistently, Real-time RT-PCR revealed that the expression of *Runx2* and *Sp7* was increased in *Bglap2*-IKK-DN cells. The induction of *Ocn* and *Ibsp* was significantly higher in *Bglap2*-IKK-DN cells than in WT cells (Fig. 3g). In contrast, the expression of *Tnfsf11* and *Tnfrsf11b* which controls osteoclast formation in these cells were not changed in *Bglap2*-IKK-DN cells compared with control cells (Fig. 3h). Additionally, we also isolated primary calvarial cells from both *Col1α1*-IKK-DN mice and WT mice. We found that calvarial cells isolated from *Col1α1*-IKK-DN mice also displayed enhanced bone matrix gene expression and bone mineralization compared with WT cells (Supplementary Fig. S4).

To further rule out a possible non-specific effect of IKK-DN, we also over-expressed p65 to determine whether NF-κB activation could reverse the effect of IKK-DN on osteoblast function. p65 is the active subunit of NF-κB which is located at the downstream of the IKK activation site12-16. If IKK-DN promoted bone formation through inhibiting NF-κB, the over-expression of p65 should be able to reverse IKK-DN-mediated enhancement. Using retroviral infection, we stably expressed p65 in *Bglap2*-IKK-DN cells as determined by Western blot analysis. The over-expression of p65 strongly suppressed matrix mineralization in *Bglap2*-IKK-DN cells (Fig. 3i). Real-time RT-PCR also confirmed that the over-

Author Manuscript Author Manuscript Author Manuscript Author Manuscript

expression of p65 inhibited the expression of *Runx2*, *Sp7*, *Alp*, *Ocn*, *Ibsp*, and *Col1α2* (Fig. 3j). On the contrary, over-expression of c-Rel and RelB in calvarial cells could not inhibit osteoblast differentiation and mineralization (Supplementary Fig. S5).

The inhibition of NF-κB reduces bone loss induced by ovariectomy

The elevated pro-inflammatory cytokines in osteoporosis have been found to stimulate bone resorption and inhibit bone formation8,30. Since these cytokines potently activate NF-κB, based on our results described above, we hypothesized that NF-κB activation secondary to sex steroid deficiency might inhibit osteoblast function in osteoporosis. To mimic the molecular pathogenesis of bone loss in postmenopausal osteoporosis in humans, the OVX mouse model has been widely used to induce estrogen deficiency and bone loss. Since the bone structure and bone mineral density of adult *Bglap2*-IKK-DN mice were identical to WT mice, these mice serve as an excellent model to test whether NF-κB activation promoted bone loss by inhibiting osteoblast function in a definitive fashion.

We sham-operated or OVXed both 3-month-old WT mice and *Bglap2*-IKK-DN mice from two founder lines. μCT revealed that trabecular bones in vertebrae and femurs from WT mice were significantly lost after OVX compared with sham-operated mice. In contrast, far less bone loss was observed in *Bglap2*-IKK-DN mice after OVX (Fig. 4a,b). Quantitative measurements indicated that whereas approximately 40% of BMD was lost in WT mice after OVX, only 12% BMD was lost in trabecular bone of femurs in *Bglap2*-IKK-DN mice after OVX (Fig. 4c). In vertebrae, while BMD was reduced over 40% in WT mice, BMD was only reduced by 20% in *Bglap2*-IKK-DN mice (Fig. 4d). Similarly, the loss of bone volume was also significantly prevented in *Bglap2*-IKK-DN mice compared with WT mice after OVX (Fig. 4c,d). Histological analysis also revealed that, while the trabecular bone mass was dramatically depleted in WT mice, a significant amount of the trabecular bone was retained in the bone marrow cavity of *Bglap2*-IKK-DN mice after OVX (Fig. 4e). To further confirm our results, we also performed OVX in *Col1*-IKK-DN mice. Compared with WT mice, bone loss in *Col1*-IKK-DN mice was also significantly reduced (Supplementary Fig. S6). Finally, we found that, while TNF inhibited bone formation induced by bone morphogenetic proteins (BMP) in WT mice, TNF inhibition of bone formation in *Bglap2*-IKK-DN mice was significantly reduced (Supplementary Fig. S7).

NF-κB activation inhibits bone formation in osteoporosis

To explore the molecular mechanism by which the inhibition of NF-κB prevented bone loss in osteoporosis, we first examined whether NF-κB was activated in osteoporosis using the specific NF-κB antibodies to detect the active form of p6523. Using anti-HA antibodies, we detected IKK-DN expression in osteoblasts of *Bglap2*-IKK-DN mice, but not of WT mice (Fig. 5a). While the active p65 in mature osteoblasts stained very weakly in *Bglap2*-IKK-DN mice, intensive p65 staining in mature osteoblasts was detected in WT mice after OVX. As a point of comparison, the active p65 was not stained in sham-operated mice (Fig. 5a).

To examine whether the inhibition of NF-κB enhanced osteoblast activity, we measured the levels of serum osteocalcin (Ocn) at 0, 1, 2, 4, 6 and 8 weeks after OVX. While a substantial increase in the levels of serum Ocn in both WT and *Bglap2*-IKK-DN mice was induced 1 to

Author Manuscript Author Manuscript Author Manuscript Author Manuscript

4 weeks after OVX, an even greater increase in the levels of serum Ocn was observed in *Bglap2*-IKK-DN mice (Fig. 5b). The levels of serum Ocn remained significantly higher in *Bglap2*-IKK-DN mice than that in WT mice 8 weeks after OVX (Fig. 5b). Moreover, in vivo dynamic labeling revealed that bone formation rates 4 weeks after OVX were significantly higher in *Bglap2*-IKK-DN mice than those in WT mice (Fig 5c). Histological analysis showed that the inhibition of NF-κB in mature osteoblasts did not affect osteoblast differentiation (Fig. 5d). There were no differences in osteoclast numbers between WT and *Bglap2*-IKK-DN mice after OVX (Fig. 5e). Moreover, the levels of serum Trap5b were increased at similar rates in WT and *Bglap2*-IKK-DN mice after OVX (Fig. 5f).

The inhibition of NF-κB promotes bone formation by up-regulating JNK/Fra-1

To explore the molecular mechanism through which NF-κB inhibition enhanced bone formation, we screened multiple signaling pathways that are involved in bone matrix protein deposition. We found that JNK activity in *Bglap2*-IKK-DN cells was greater than WT cells two weeks after induction of osteoblast differentiation *in vitro* (Fig. 6a, second panel). The appearance of increased JNK activities was consistent with the induction of IKK-DN (top panel). In contrast, there were no significant differences in p38 activities between *Bglap2*-IKK-DN and WT cells (Fig. 6b). Previously, NF-κB was found to negatively regulate JNK activity, and inhibition of NF-κB leads to prolonged JNK activation31-33. Thus, increased JNK activities were likely due to the inhibition of NF-κB in differentiated osteoblasts.

It is known that the activation of JNK stimulates AP-1 transcription7,34. Genetic studies established that several members of AP-1 family members such as Fra-1 (encoded by *Fosl1*) and FosB play essential roles in bone formation after birth35-37. Thus, we first explored whether *Fosl1* and *Fosb* were differentially induced in *Bglap2*-IKK-DN cells relative to WT cells. Real-time RT-PCR revealed that *Fosl1* expression was significantly higher in *Bglap2*-IKK-DN cells compared with WT cells upon induction (Fig. 6c). Of note, the difference might be underestimated due to cell heterogeneicity *in vitro*. In contrast, RT-PCR showed that there was no difference in *Fosb* and *deltaFosb* in both *Bglap2*-IKK-DN cells and WT cells (Fig. 6d). Additionally, other AP-1 family members including *Jun, Junb, Jund* and *Fos* were detected at similar levels in both *Bglap2*-IKK-DN cells and control cells (Fig. 6e). Moreover, Western blot analysis also confirmed that Fra-1 proteins were enhanced in *Bglap2*-IKKDN cells compared with control cells (Fig. 6a). The JNK inhibitor SP600125 also inhibited the expression of Fra-1, suggesting that Fra-1 expression was dependent on JNK activation (Fig. 6f).

To determine if Fra-1 played a role in osteoblast function, we utilized a siRNA strategy to knock-down *Fosl1*. While shRNA *Fosl1*-1 reduced Fra-1 levels by only 20%, shRNA *Fosl1*-2 reduced over 90% of Fra-1 levels in osteoblasts as determined by Western blot analysis (Fig. 6g). Consistently, shRNA *Fosl1*-2 more significantly inhibited bone matrix mineralization of *Bglap2*-IKK-DN cells in vitro (Fig. 6h). Real-Time RT-PCR revealed that shRNA *Fosl1*-2 substantially suppressed the expression of bone matrix genes including *Ocn, Ibsp*, and *Col1α2* (Fig. 6i). To further determine whether enhanced Fra-1 expression was responsible for preventing bone loss in OVX mice, we also performed immunostaining to examine Fra-1 expression in osteoblasts *in vivo*. While the basal level of Fra-1 was similar

Author Manuscript Author Manuscript Author Manuscript Author Manuscript

in both sham-operated WT and *Bglap2*-IKK-DN mice, the intensive Fra-1 staining was found in osteoblasts localized on the bone surfaces of *Bglap2*-IKK-DN mice relative to WT mice after OVX (Fig. 6j).

DISCUSSION

Post-menopausal osteoporosis is a common debilitating metabolic disease that represents a major public burden to human health. There is a relative deficit in bone formation in osteoporosis. In this study, NF-κB is identified as a critical factor responsible for inhibiting bone formation in a model of osteoporosis. The suppression of NF-κB in differentiated osteoblasts prevents osteoporotic bone loss by maintaining osteoblast function. Considering the well-established role of NF-κB in osteoclast activation and bone resorption, our results suggest that targeting NF-κB in the treatment for osteoporosis and inflammatory bone disorders will not only suppress bone resorption, but also promote bone formation which is important for rebuilding bone mass.

According to our immunostaining studies, NF-κB in differentiated osteoblasts is abnormally activated in OVX-induced osteoporosis. There are two primary mechanisms which may promote NF-κB activation in differentiated osteoblasts. First, estrogen receptor (ER) has been found to directly inhibit NF-κB transcription in a ligand-dependent fashion by interacting with NF-κB38. Since ER is expressed in osteoblasts, estrogen may negatively regulate NF-κB activities under the physiological conditions. However, during the pathogenesis of osteoporosis, this negative regulation may be diminished due to lack of estrogen, resulting in the elevation of basal NF-κB activities in osteoblasts. Second, the pro-inflammatory cytokines, including TNF, IL-1, IL-6 and IL-7, have been found to be highly expressed by T cells and other cells in osteoporosis8. These cytokines can potently stimulate NF-κB activities in osteoblasts. Previously, most studies focused on how pro-inflammatory cytokines activate NF-κB to induce osteoclast formation and activation18. However, it has long been known that the pro-inflammatory cytokines also inhibited osteoblast differentiation and bone formation in osteoporosis, arthritis, periodontitis and multiple myeloma by unknown mechanims8,9,30,39. Our results suggest that these cytokines activate NF-κB to suppress osteoblast function, thereby inhibiting bone formation. Our *in vitro* studies revealed that the inhibition of NF-κB leads to enhanced Fra-1 expression in differentiated osteoblasts. Previously, the loss and gain of function studies in mice have demonstrated that Fra-1 is an essential factor for bone matrix deposition or bone formation35,37. However, although Fra-1 is an important target, it remains possible that NF-κB may regulate other molecules to inhibit bone formation. Taken together, based on our studies described here and other works on osteoclasts, we propose a new role of NF-κB in osteoporosis: the activation of NF-κB due to sex steroid deficiency not only promotes osteoclast activation and bone resorption, but simultaneously inhibits osteoblast function, thus limiting the compensatory bone formation from maintaining bone homeostasis (Supplementary Fig. S8).

Author Manuscript Author Manuscript Author Manuscript Author Manuscript

METHODS

Cell Culture

We isolated primary calvarial cells from new-born mice and cultured in α-MEM with 10% FBS. To induce osteoblastic differentiation, we grew cells in differentiation-inducing media containing 100 μg/ml ascorbic acid, 2 mM β-glycerophosphate and 1 μM dexamethasone for 1, 2 and 3 weeks. After induction, we fixed cells with 70% EOTH and stained with an ALP staining kit according to the manufacturer's protocol (Sigma-Aldrich). For detecting mineralization, we induced cells for 2 to 3 weeks, fixed with 70% ETOH and stained with 2% Alizarin red (Sigma-Aldrich).

Western Blot Analysis, EMSA and Real-time RT-PCR

We performed Western blot analysis and EMSA as described previously23. We obtained the primary antibodies from the following sources: polyclonal antibody to IκBα (Santa Cruz); polyclonal antibody to p65 (Rockland); monoclonal antibody to α-tubulin (Sigma); and polyclonal antibody to Runx-2 (Oncogene Research Products). We extracted total RNA using Trizol (Invitrogen). We synthesized 2-μg aliquots of RNAs using random hexamers and reverse transcriptase (Invitrogen). We performed the Real-time PCR reactions using the QuantiTect SYBR Green PCR kit (Qiangen) and Icycler iQ Multi-color Real-time PCR Detection System. The primer sequences are listed in Supplementary Methods.

Generation of Transgenic Mice

We used the plasmid pGL647 contains the *Bglap2* promoter to specifically drive osteoblast-specific gene expression in vivo26. We subcloned human IKK-DN cDNA into pGL647. The fragments of *Bglap2*-IKK-DN transgene were purified and microinjected into (C57BL/6 X SJL) F2 mouse oocytes (Charles River Laboratories) and surgically transferred to pseudopregnant C57BL/6 dams by the University of Michigan Transgenic Animal Model Core. We screened the founders by PCR using mouse tail genomic DNA and confirmed them using Southern blot analysis. We bred two transgenic founder animals into C57BL/6 mice for six generations to obtain a defined genetic background. We OVXed 3-month-old transgenic and WT mice to induce osteoporosis. 2 months after operation, we sacrificed mice and harvested tibiae, femurs and vertebrae for histological and μCT analysis. We collected blood samples and isolated serums for serology. We measured serum TRAP5b a mouse TRAP™ assay kit (SBA Sciences) and OCN with an OCN ELISA kit (Biomedical Technologies Inc.). The University Committee on Use and Care of Animals at the University of Michigan and/or the Animal Research Committee at the University of California, Los Angeles approved all mouse protocols.

Bone Histological and Morphological Analysis

We stained skeleton from newborn pups with alizarin red and alcian blue as previously described28. For histological analysis, we sacrificed mice at the age of 2, 4 and 8 weeks and 6 months, and fixed femurs and vertebrae in 10% neutral buffered formalin. For immunostaining, we performed antigen retrieval by pressure cooking in a Decloaking chamber (Biocare Medical) in citrate buffer (2.1 g/L citric acid, pH 6.0) at 120 °C for 20

Author Manuscript Author Manuscript Author Manuscript Author Manuscript

min. We incubated sections with polyclonal antibodies against Fra-1 (Santa Cruz; 1:100), polyclonal antibodies against the active form of p65 (Rockland Inc; 1: 100), monoclonal and polyclonal antibodies against HA (1:100), and polyclonal antibodies against phosphor-JNK (Cell Signaling; 1: 200) at 4 °C overnight. We then incubated sections with horseradish perioxidase-labeled polymer for 30 min, detected the immunocomplexes with AEC^+ chromogen (Dako EnVision System) and counterstained with hematoxylin as described previously23. For examination of bone formation, we injected mice with calcein seven days apart and sacrificed two days after the final injection. We isolated tibiae, fixed them in ethanol, and embedded them in methyl methacrylate. We prepared 8-μm longitudinal sections with microtome. We evaluated sections by fluorescent microscope or stained with 1% toluidine blue, or von Kossa reagents. For osteoclast detection, we stained the sections with TRAP activities using a leukocyte acid phosphatase staining kit (Sigma-Aldrich). We measured bone parameters of femurs, tibiae and vertebrae using computer-assisted histomorphometry using Image Pro Plus 4.5 (Media Cybernetics) and SPOT 4.0 software (Diagnostic Instruments).

We set the microradiography unit to 80 kV and 100 μA and scanned specimens at a 8.93 m voxel resolution on an EVS Corporation μCT scanner, with a total of 667 slices per scan. We generated a three-dimensional reconstruction with GEMS MicroView software from the set of scans. We defined the regions of interest (ROI) as the areas between 0.3 mm and 0.6 mm proximal to the growth plate in the distal femurs in order to include the secondary trabecular spongiosa. In vertebral bodies, we selected a cylinder fitting in the whole central regions of the trabecular bone as ROI. We used a fixed threshold (600) to extract the mineralized bone phase and actual bone volume, and calculated BMD.

Supplementary Material

Refer to Web version on PubMed Central for supplementary material.

ACKNOWLEDGEMENTS

We thank Dr. J. Adams for valuable advices and Drs. G. Karsenty and T. Gilmore for reagents. This work was supported by National Institute of Dental and Craniofacial Research Grants (DE17684, DE019412 and DE1016513 to C.Y.W.), and National Institute of Diabetes and Kidney Disease Grants.

REFERENCES

1. Wagner EF, Karsenty G. Genetic control of skeletal development. Curr. Opin. Genet. Dev. 2001; 11:527–532. [PubMed: 11532394]
2. Khosla S, Westendorf JJ, Oursler MJ. Building bone to reverse osteoporosis and repair fractures. J Clin. Invest. 2008; 118:421–428. [PubMed: 18246192]
3. Zaidi M. Skeletal remodeling in health and disease. Nat Med. 2007; 13:791–801. [PubMed: 17618270]
4. Zelzer E, Olsen BR. Multiple roles of vascular endothelial growth factor (VEGF) in skeletal development, growth, and repair. Curr Top Dev Biol. 2005; 65:169–187. [PubMed: 15642383]
5. Kronenberg HM. *Twist* Genes Regulate Runx2 and Bone Formation. Dev. Cell. 2004; 6:317–318. [PubMed: 15030754]
6. Lian JB, et al. Regulatory controls for osteoblast growth and differentiation: role of Runx/Cbfa/AML factors. Crit. Rev. Eukaryot. Gene Expr. 2004; 14:1–41. [PubMed: 15104525]

Author Manuscript Author Manuscript Author Manuscript Author Manuscript

7. Clowes JA, Riggs BL, Khosla S. The role of the immune system in the pathophysiology of osteoporosis. Immunol Rev. 2005; 208:207–227. [PubMed: 16313351]
8. Raisz LG. Pathogenesis of osteoporosis: concepts, conflicts, and prospects. J Clin. Inv. 2005; 115:3318–3325.
9. Weitzmann MN, Pacifici R. Estrogen deficiency and bone loss: an inflammatory tale. J Clin. Inv. 2006; 116:1186–1194.
10. Teitelbaum SL, Ross FP. Genetic regulation of osteoclast development and function. Nat. Rev. Genet. 2003; 4:638–649. [PubMed: 12897775]
11. Khosla S, Riggs BL. Pathophysiology of age-related bone loss and osteoporosis. Endocrinol Metab Clin North Am. 2005; 34:1015–1030. [PubMed: 16310636]
12. Ghosh S, Karin M. Missing pieces in the NF-kappaB puzzle. Cell. 2002; 109:S81–96. [PubMed: 11983155]
13. Chen ZJ. Suppression of tumor necrosis factor-mediated apoptosis by nuclear factor kappaB-independent bone morphogenetic protein/Smad signaling. Nat. Cell Biol. 2005; 7:758–765. [PubMed: 16056267]
14. Huang TT, et al. Sequential modification of NEMO/IKKγ by SUMO-1 and ubiquitin mediates NF-κB activation by genotoxic stress. Cell. 2003; 115:565–576. [PubMed: 14651848]
15. Li Q, Verma IM. NF-kappaB regulation in the immune system. Nat. Rev. Immunol. 2002; 2:725–734. [PubMed: 12360211]
16. Silverman N, Maniatis T. NF-kappaB signaling pathways in mammalian and insect innate immunity. Genes Dev. 2000; 15:2321–2342. [PubMed: 11562344]
17. Guttridge DC, et al. NF-κB activation induces the loss of MyoD mRNA: implications for cytokine-induced skeletal muscle dysfunction and cachexia. Science. 2000; 289:2363–2366. [PubMed: 11009425]
18. Jimi E, et al. Selective inhibition of NF-κB blocks osteoclastogenesis and prevents inflammatory bone destruction in vivo. Nat. Med. 2004; 10:617–624. [PubMed: 15156202]
19. Ruocco MG, et al. IκB kinase (IKK)β, but not IKKα, is a critical mediator of osteoclast survival and is required for inflammation-induced bone loss. J. Exp. Med. 2005; 201:1677–1687. [PubMed: 15897281]
20. Tang ED, et al. A role for NF-kappaB essential modifier/IkappaB kinase-gamma (NEMO/IKKgamma) ubiquitination in the activation of the IkappaB kinase complex by tumor necrosis factor-alpha. J Biol. Chem. 2003; 278:37297–305. [PubMed: 12867425]
21. Yang F, et al. The zinc finger mutation C417R of I-kappa B kinase gamma impairs lipopolysaccharide- and TNF-mediated NF-kappa B activation through inhibiting phosphorylation of the I-kappa B kinase beta activation loop. J Immunol. 2004; 172:2446–2452. [PubMed: 14764716]
22. Wang C-Y, et al. TNF- and cancer therapy-induced apoptosis: potentiation by inhibition of NF-κB. Science. 1996; 274:784–787. [PubMed: 8864119]
23. Park BK, et al. NF-kappaB in breast cancer cells promotes osteolytic bone metastasis by inducing osteoclastogenesis via GM-CSF. Nat Med. 2007; 13:62–69. [PubMed: 17159986]
24. Wang C-Y, et al. Control of inducible chemoresistance: enhanced anti-tumor therapy via increased apoptosis through inhibition of NF-κB. Nat. Med. 1999; 5:412–417. [PubMed: 10202930]
25. Ducy P, et al. A Cbfa1-dependent genetic pathway controls bone formation beyond embryonic development. Genes Dev. 1999; 13:1025–1036. [PubMed: 10215629]
26. Frendo J, et al. Functional hierarchy between two OSE2 elements in the control of osteocalcin gene expression *in vivo*. J. Biol. Chem. 1998; 273:30509–30516. [PubMed: 9804819]
27. Billic-Curcic I, et al. Visualizing levels of osteoblasts differentiation by two-color promoter-GFP strategy: Type I collagen-GFPcyan and osteocalcin-GFPtpz. Genesis. 2005; 43:87–98. [PubMed: 16149065]
28. Ge C, et al. Critical role of the extracellular signal-regulated kinase-MAPK pathway in osteoblast differentiation and skeletal development. J Cell Biol. 2007; 176:709–718. [PubMed: 17325210]
29. Schmidt-Ullrich R, et al. NF-kappaB activity in transgenic mice: developmental regulation and tissue specificity. Development. 1996; 122:2117–2128. [PubMed: 8681793]

Author Manuscript Author Manuscript Author Manuscript Author Manuscript

30. Li YP, Stashenko P. Characterization of a tumor necrosis factor-responsive element which down-regulates the human osteocalcin gene. Mol. Cell. Biol. 1993; 13:3714–3721. [PubMed: 8388544]
31. De Smaele E, et al. Induction of gadd45ß by NF-κB downregulates pro-apoptotic JNK signaling. Nature. 2001; 414:308–313. [PubMed: 11713530]
32. Tang G, et al. Inhibition of JNK activation through NF-kappaB target genes. Nature. 2001; 414:313–317. [PubMed: 11713531]
33. Reuther-Madrid JY, et al. The p65/RelA subunit of NF-κB suppresses the sustained, antiapoptotic activity of Jun kinase induced by tumor necrosis factor. Mol. Cell. Biol. 2002; 22:8175–8183. [PubMed: 12417721]
34. Yamashita M, et al. Ubiquitin ligase smurf1 controls osteoblast activity and bone homeostasis by targeting MEKK2 for degradation. Cell. 2005; 121:101–113. [PubMed: 15820682]
35. Jochum W, et al. Increased bone formation and osteosclerosis in mice overexpressing the transcription factor Fra-1. Nat. Med. 2000; 6:980–984. [PubMed: 10973316]
36. Sabatakos G, et al. Overexpression of DeltaFosB transcription factor(s) increases bone formation and inhibits adipogenesis. Nat. Med. 2000; 6:985–990. [PubMed: 10973317]
37. Eferl R, et al. The Fos-related antigen Fra-1 is an activator of bone matrix formation. EMBO J. 2004; 23:2789–2799. [PubMed: 15229648]
38. Harnish DC. Estrogen receptor ligands in the control of pathogenic inflammation. Cur. Opin. Inv. Drug. 2006; 7:997–1001.
39. Pearse RN. Wnt antagonism in multiple myeloma: a potential cause of uncoupled bone remodeling. Clin. Cancer Res. 2006; 12:6274s–6278s. [PubMed: 17062713]

Author Manuscript Author Manuscript Author Manuscript Author Manuscript

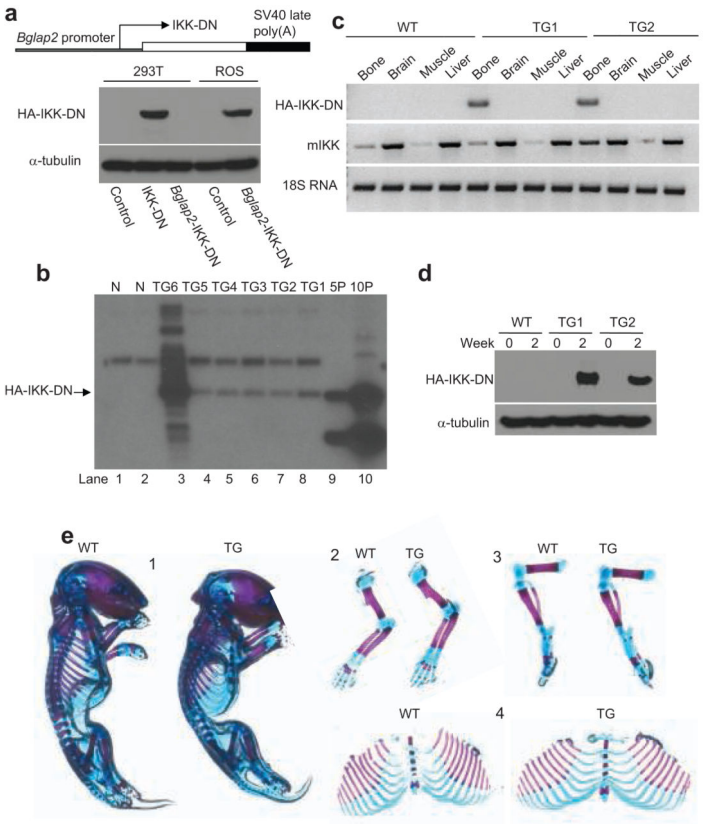

Fig. 1. Generation of transgenic mouse specifically expressing IKK-DN in differentiated osteoblasts

(**a**) Generation of *Bblap2*-dependent IKK DN construct. Cells were probed with anti-HA monoclonal antibodies. α-tubulin was used as a loading control. (**b**) Generation of *Bblap2*-IKK-DN transgenic mice. Genomic DNAs from tail tissues were probed with ^{32}P-labeled human IKK-DN cDNA probes. N, Genomic DNAs from WT mice; TG, *Bblap2*-IKK-DN transgenic mouse; 5P, 5 copies of human IKK-DN cDNA; 10P, 10 copies of human IKK-DN cDNA. (**c**) IKK-DN was specifically expressed in bone tissues. Total RNA from long bones, brain, muscle and liver examined with RT-PCR. WT, wild type mouse; TG1, *Bblap2*-IKK-DN founder line 1; TG2, *Bblap2*-IKK-DN founder line 2. (**d**) IKK-DN was induced in differentiated osteoblasts. Differentiated cells were probed with anti-HA antibodies. α-tubulin was used as a loading control. TG1, *Bblap2*-IKK-DN transgenic mouse line 1; TG2, *Bblap2*-IKK-DN transgenic mouse line 2. (**e**) Normal skeleton of newborn WT and *Bblap2*-IKK-DN mice. Whole mounts of newborn skeletons were stained with alcian blue and alizarin red. 1, whole skeleton; 2, upper extremities; 3, hind limbs; 4, Rib.

Author Manuscript Author Manuscript Author Manuscript Author Manuscript

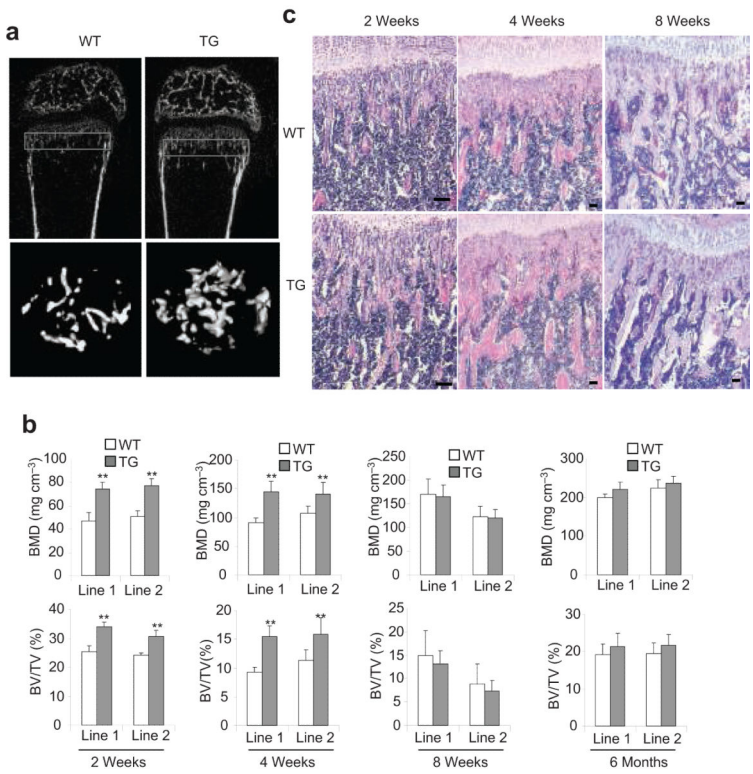

Author Manuscript Author Manuscript Author Manuscript Author Manuscript

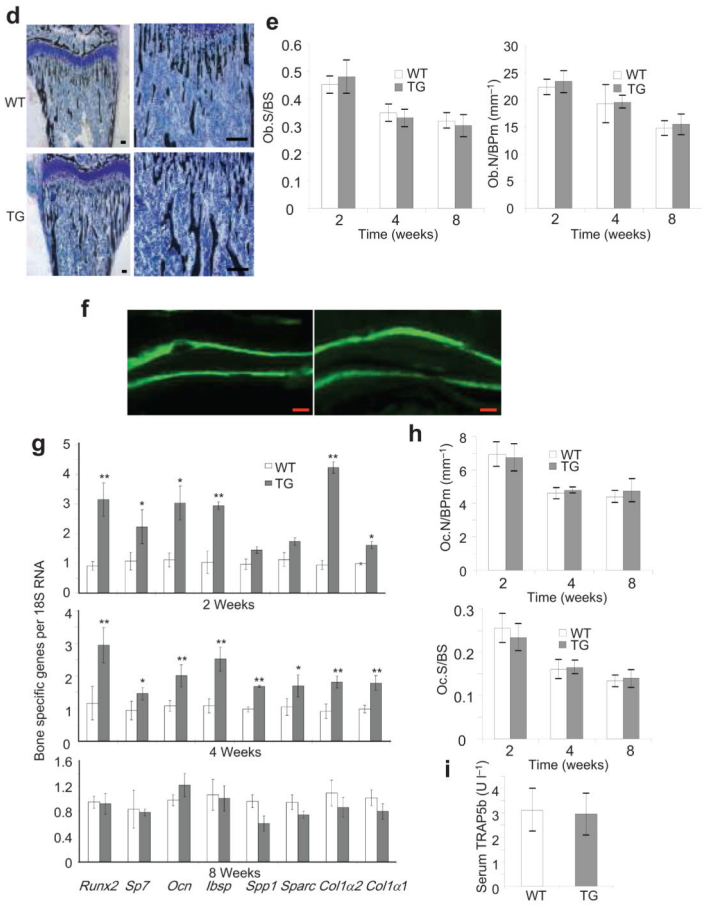

Fig. 2. The inhibition of NF-κB by IKK-DN in mature osteoblasts enhanced bone formation in young mice

(**a**) μCT images of the trabecular bone of femurs from WT and *Bblap2*-IKK-DN mice. (**b**) Enhanced bone formation in young *Bblap2*-IKK-DN mice. Morphometric properties of femurs from different ages of both WT and *Bblap2*-IKK-DN mice were measured by μCT. The results are the average values from 12-15 mice per group and presented as mean ± s.d. $^{**}P < 0.01$. BMD, bone mineral density; BV/TV, trabecular bone volume per tissue volume; WT, wild type mice; TG, *Bblap2*-IKK-DN mice. (**c**) H&E analysis of femurs from WT and *Bblap2*-IKK-DN mice. Scale bar, 50 μm. (**d**) von Kossa staining of tibiae from WT and *Bblap2*-IKK-DN mice. Scale bar, 50 μm. (**e**) Osteoblast numbers in both WT and *Bblap2*-IKK-DN mice. The results are the average value from 12-15 mice per group and presented as mean ± s.d. (**f**) Enhanced bone formation in *Bblap2*-IKK-DN mice as determined by calcein double-labeling. Four-week-old mice were labeled with calcein. The results are the average value from 10 mice per group. $^{**}P < 0.01$. Scale bar, 10 μm. (**g**) The expression of bone matrix genes was enhanced in young *Bblap2*-IKK-DN mice. Total RNAs were examined with Real-time RT-PCR. $^{*}P < 0.05$; $^{**}P < 0.01$. (**h**) Osteoclast numbers in both WT and *Bblap2*-IKK-DN mice. The results are the average value from 12-15 mice per group and presented as mean ± s.d. Oc.S/BS, osteoclast surface per bone surface; Oc.N/BPm (mm^{-1}); osteoclast number per bone perimeter. (**i**)Serum Trap5b in both WT and *Bblap2*-

IKK-DN mice. The results are the average values from 12-15 mice per group and presented as mean ± s.d.

Author Manuscript Author Manuscript Author Manuscript Author Manuscript

Author Manuscript
Author Manuscript
Author Manuscript
Author Manuscript

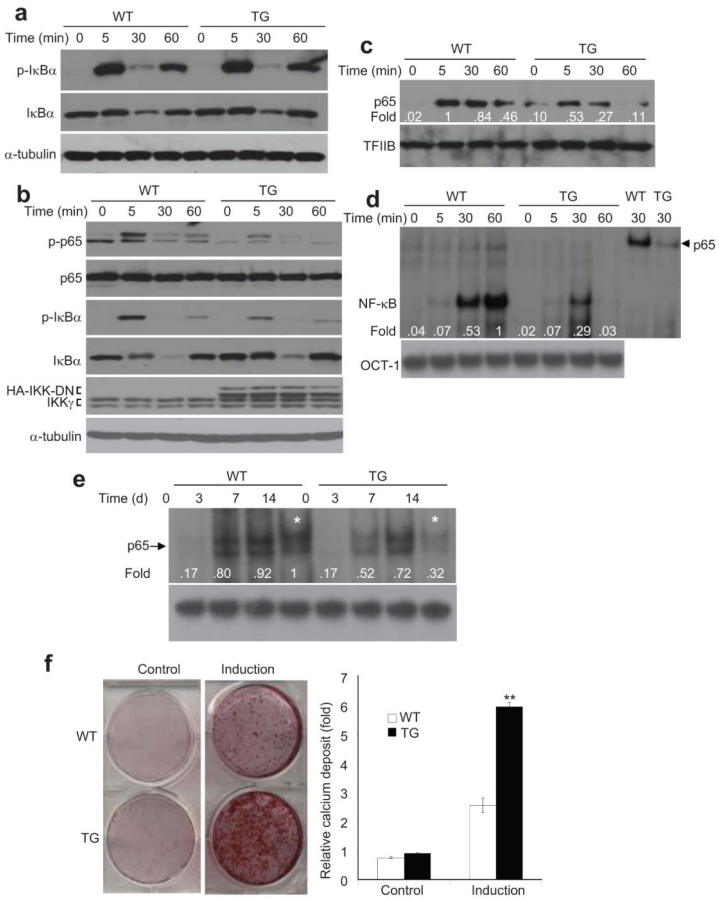

Author Manuscript Author Manuscript Author Manuscript Author Manuscript

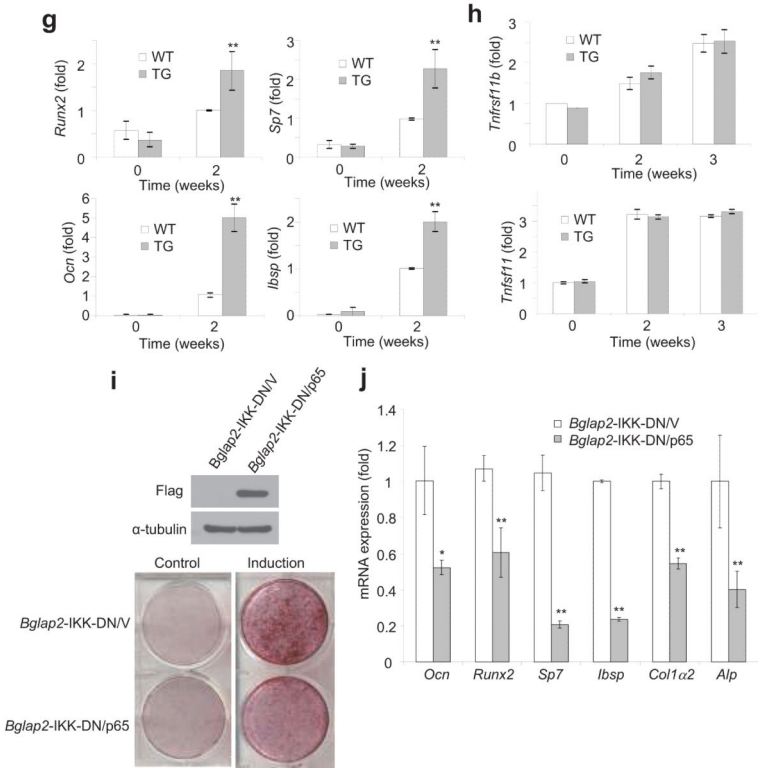

Fig. 3. The inhibition of NF-κB in mature osteoblasts enhances bone formation in a cell-autonomous fashion

(**a**) NF-κB signaling was intact in un-differentiated osteoblast progenitors. The phosphorylation and degradation of IκBα were examined by Western blot analysis. (**b**) IKK-DN inhibited IKKβ activities in differentiated osteoblast cells isolated from *Bblap2*-IKK-DN mice. Calvarial cells were induced to differentiate for 10 days. After induction, cells were treated with TNF. The phosphorylation and degradation of IκBα and p65 phosphorylation were examined by Western blot analysis. The induction of IKK-DN was probed with anti-IKKγ. (**c**) IKK-DN blocked the nuclear translocation of p65 induced by TNF. The level of nuclear p65 was examined by Western blot analysis. (**d**) IKK-DN blocked TNF-induced NF-κB-binding activities. (**e**) IKK-DN blocked NF-κB in differentiated osteoblasts. Calvarial cells from both WT and *Bglap2*-IKK-DN mice were induced to differentiate for the indicated periods and the nuclear proteins were isolated. Nuclear proteins were incubated ^{32}P-labeled κB probed. (**f**) The inhibition of NF-κB in differentiated osteoblasts enhanced mineralization. The experiments were performed in duplicate. The results represent average value from three independent experiments. $^{**}P < 0.01$. (**g**) The inhibition of NF-κB enhanced the expression of *Runx2, Sp7, Ocn* and *Ibsp* as determined by Real-time RT-PCR. $^{**}P < 0.01$. (**h**) The inhibition of NF-κB in differentiated osteoblasts did not affect the expression of *Tnfsf11* and *Tnfrsf11b*. (**i**) Over-expression of p65 in calvarial cells isolated from *Bglap2*-IKK-DN mice inhibited mineralization. p65 was examined by Western blot analysis. The mineralization was examined by Alizarin red staining. (**j**) p65 overcame IKK-DN effects on bone matrix gene expression. Cells were induced to differentiate and total RNAs were examined by Real-time RT-PCR. $^{*}P < 0.05$; $^{**}P < 0.01$.

Author Manuscript Author Manuscript Author Manuscript Author Manuscript

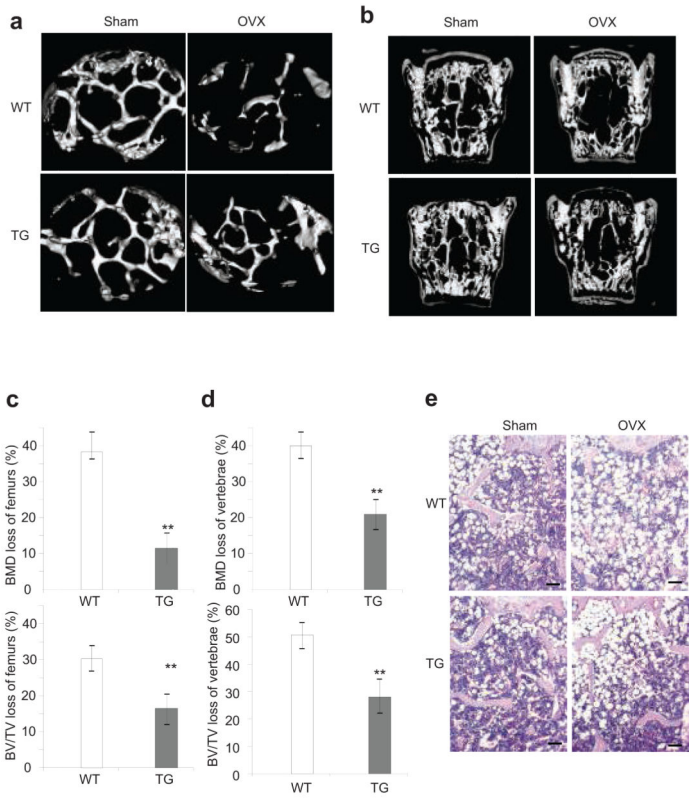

Fig. 4. The inhibition of NF-κB in mature osteoblasts prevents trabecular bone loss induced by OVX in adult mice

(**a**) The inhibition of NF-κB prevented trabecullar bone loss of femurs in adult mice as determined by μCT. (**b**) The inhibition of NF-κB prevented trabecullar bone loss of vertabrae as determined by μCT. (**c** and **d)** Quantitative measurement of bone loss in vertebrae and femurs by μCT. The results are average values from 12-15 mice per group and presented as mean ± s.d. $^{**}P < 0.01$. (**e**) The inhibition of NF-κB prevented trabecular bone loss of femurs as determined by the histological analysis. Scale bar, 100 μm.

Author Manuscript Author Manuscript Author Manuscript Author Manuscript

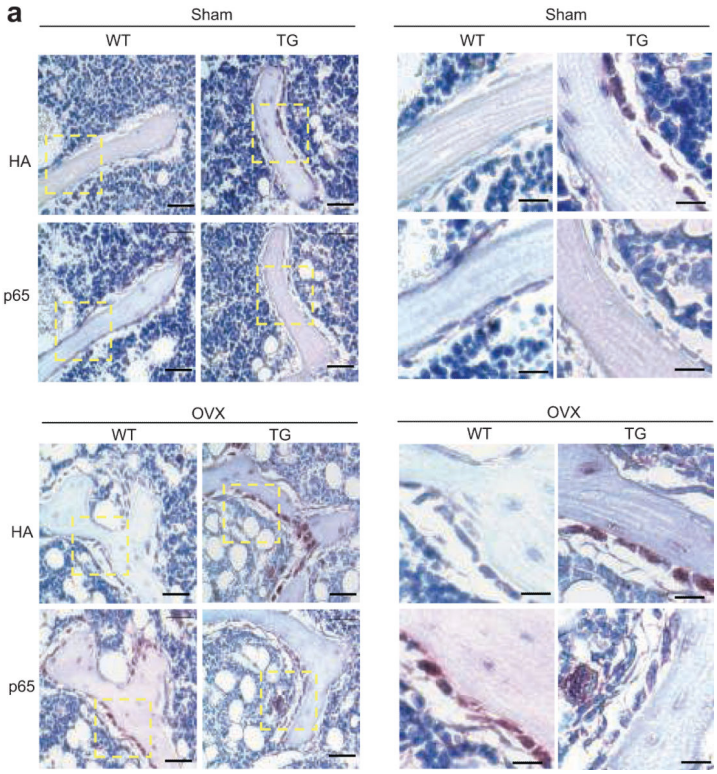

Author Manuscript Author Manuscript Author Manuscript Author Manuscript

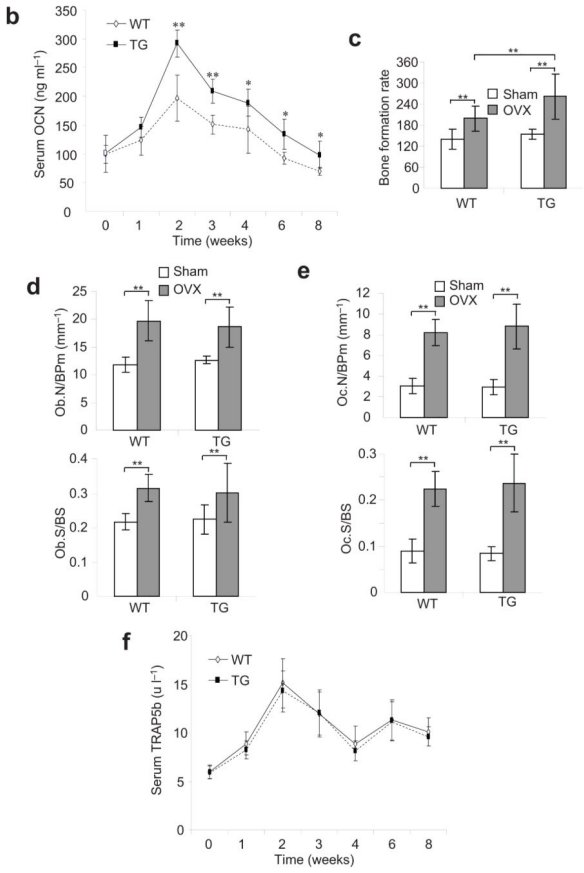

Fig. 5. The inhibition of NF-κB in mature osteoblasts prevents bone loss by maintaining osteoblast functions in adult mice

(**a**) NF-κB in osteoblasts was activated during OVX-induced bone loss. 3-month-old WT and *Bblap2*-IKK-DN mice were OVXed or sham-operated. Femurs from mice were sectioned and stained with anti-active form of p65 and anti-HA. Scale bars at left panel, 50 μm; scale bars at right panel, 20 μm. (**b**) The inhibition of NF-κB enhanced osteoblast activities in osteoporosis. Serum Ocn was measured using an Ocn ELISA kit. The results are average values from 6-8 mice per group and presented as mean values ± s.d. **P* < 0.05; ***P* < 0.01. (**c**) The inhibition of NF-κB enhanced bone formation in osteoporosis. The bone formation rate in mice was determined 4 weeks after operation. The results are average values from 6-8 mice per group and presented as mean values ± s.d. **P* < 0.01. (**d**) The inhibition of NF-κB did not affect osteoblast numbers. Osteoblast numbers in mice were examined 4 weeks after operation. The results are average values from 6-8 mice per group and presented as mean values ± s.d. (**e**) The inhibition of NF-κB in osteoblasts did not affect osteoclast formation. Osteoclast numbers in mice were examined 4 weeks after operation. The results are average values from 6-8 mice per group and presented as mean values ± s.d. (**f**) The inhibition of NF-κB in osteoblasts did not inhibit bone resorption in osteoporosis. Mice were operated and sacrificed at 0, 1, 2, 3, 4, 6 and 8 weeks. Serum Trap5b levels were measured using a mouse TRAP™ assay kit. The results are average values from 6-8 mice per group and presented as mean values ± s.d.

Author Manuscript Author Manuscript Author Manuscript Author Manuscript

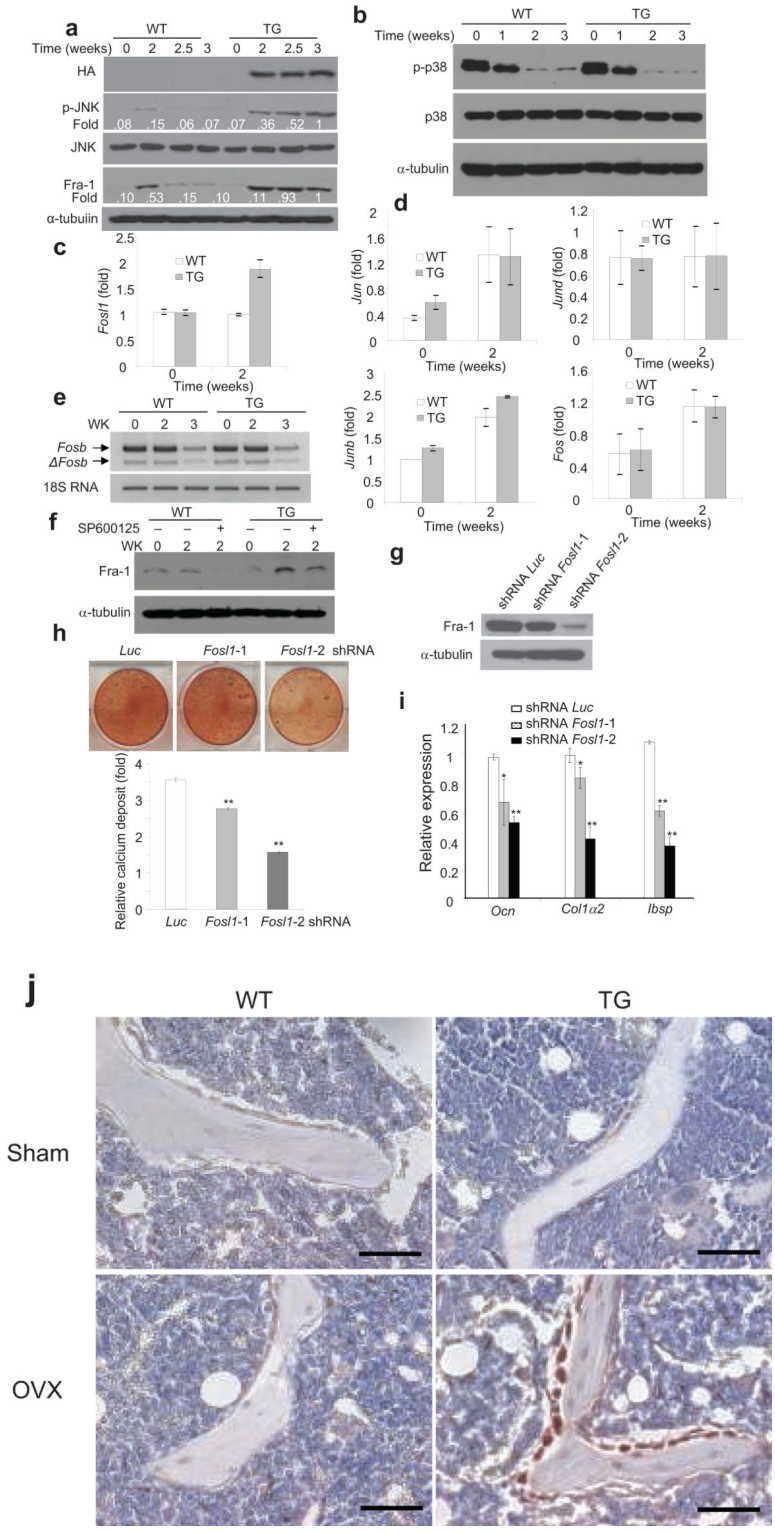

Fig. 6. The inhibition of NF-κB promoted osteoblast activities by inducing Fra-1 expression

(**a**) The inhibition of NF-κB enhanced JNK activities and Fra-1 expression in differentiated osteoblasts. Calvarial cells from both WT and *Bblap2*-IKK-DN mice were induced to

Author Manuscript Author Manuscript Author Manuscript Author Manuscript

differentiate and the JNK phosphorylation and Fra-1 expression were examined by Western blot analysis. α-tubulin was used as a loading control. (**b**) The inhibition of NF-κB did not affect p38 activation. (**c**) The inhibition of NF-κB in mature osteoblasts enhanced *Fosl1* as determined by Real-time RT-PCR. ***P* < 0.01. (**d**) The inhibition of NF-κB in mature osteoblasts did not affect the expression of *Fosb* and *deltaFosb* as determined by RT-PCR. (**e**) The inhibition of NF-κB in mature osteoblasts did not affect the expression of *Jun*, *Junb*, *Jund* and *Fos* as determined by Real-time RT-PCR. (**f**) The inhibition of JNK suppressed *Fosl1*. Whole cell lysates were examined by Western blot analysis. (**g**) The knock-down of *Fosl1* by shRNA. Whole cell lysates were probed with anti-Fra-1 antibodies. α-tubulin was used as a loading control. (**h**) The knock-down of *Fosl1* significantly decreased mineralization. **P* < 0.05; ***P* < 0.01. (**i**) The knock-down of *Fosl1* significantly reduced the expression of bone matrix genes. **P* < 0.05; ***P* < 0.01. (**j**) The inhibition of NF-κB in mature osteoblasts enhanced Fra-1 expression in OVX mice. The femoral sections from WT and *Bblap2*-IKK-DN mice after OVX or sham operation were stained with anti-Fra-1 antibodies. Scale bars, 50 μm.